

Measurement of the Λ_b^0 , Ξ_b^- , and Ω_b^- Baryon Masses

R. Aaij *et al.**

(LHCb Collaboration)

(Received 5 February 2013; published 2 May 2013)

Bottom baryons decaying to a J/ψ meson and a hyperon are reconstructed using 1.0 fb^{-1} of data collected in 2011 with the LHCb detector. Significant $\Lambda_b^0 \rightarrow J/\psi \Lambda$, $\Xi_b^- \rightarrow J/\psi \Xi^-$ and $\Omega_b^- \rightarrow J/\psi \Omega^-$ signals are observed and the corresponding masses are measured to be $M(\Lambda_b^0) = 5619.53 \pm 0.13(\text{stat.}) \pm 0.45(\text{syst.}) \text{ MeV}/c^2$, $M(\Xi_b^-) = 5795.8 \pm 0.9(\text{stat.}) \pm 0.4(\text{syst.}) \text{ MeV}/c^2$, $M(\Omega_b^-) = 6046.0 \pm 2.2(\text{stat.}) \pm 0.5(\text{syst.}) \text{ MeV}/c^2$, while the differences with respect to the Λ_b^0 mass are $M(\Xi_b^-) - M(\Lambda_b^0) = 176.2 \pm 0.9(\text{stat.}) \pm 0.1(\text{syst.}) \text{ MeV}/c^2$, $M(\Omega_b^-) - M(\Lambda_b^0) = 426.4 \pm 2.2(\text{stat.}) \pm 0.4(\text{syst.}) \text{ MeV}/c^2$. These are the most precise mass measurements of the Λ_b^0 , Ξ_b^- and Ω_b^- baryons to date. Averaging the above Λ_b^0 mass measurement with that published by LHCb using 35 pb^{-1} of data collected in 2010 yields $M(\Lambda_b^0) = 5619.44 \pm 0.13(\text{stat.}) \pm 0.38(\text{syst.}) \text{ MeV}/c^2$.

DOI: [10.1103/PhysRevLett.110.182001](https://doi.org/10.1103/PhysRevLett.110.182001)

PACS numbers: 14.20.Mr

Hadrons are systems bound by the strong interaction, described at the fundamental level by quantum chromodynamics (QCD). While QCD is well understood at high energy in the perturbative regime, low-energy phenomena such as the binding of quarks and gluons within hadrons are more difficult to predict. Several models and techniques, such as constituent quark models or lattice QCD calculations, attempt to reproduce the spectrum of the measured hadron masses (for a review, see Ref. [1]). While the masses of all expected ground-state mesons are now well measured, baryon data are still sparse. In particular, only six out of the sixteen b -baryon ground states predicted by the quark model have been observed so far [2]. A complete and reliable experimental mass spectrum would allow for precision tests of a variety of QCD models [3].

The mass measurement of the heaviest observed b baryon, the Ω_b^- state with bss valence quark content, is of particular interest. While both the D0 and CDF collaborations have claimed the observation of the $\Omega_b^- \rightarrow J/\psi \Omega^-$ decay, the reported mass values, $6165 \pm 10(\text{stat.}) \pm 13(\text{syst.}) \text{ MeV}/c^2$ from D0 [4] and $6054.4 \pm 6.8(\text{stat.}) \pm 0.9(\text{syst.}) \text{ MeV}/c^2$ from CDF [5], differ by more than 6 standard deviations. On the other hand, there is good agreement between the mass measurements of the Ξ_b^- (bsd) baryon, which has also been observed by D0 [6] and CDF [7] in the $\Xi_b^- \rightarrow J/\psi \Xi^-$ mode and, more recently, by CDF [8] in the $\Xi_b^- \rightarrow \Xi_c^0 \pi^-$ mode. These measurements average to $5791.1 \pm 2.2 \text{ MeV}/c^2$ [2].

This Letter presents mass measurements of the weakly decaying Λ_b^0 (bud), Ξ_b^- and Ω_b^- baryons using the decay

modes $\Lambda_b^0 \rightarrow J/\psi \Lambda$, $\Xi_b^- \rightarrow J/\psi \Xi^-$ and $\Omega_b^- \rightarrow J/\psi \Omega^-$ (charge-conjugated modes are implied throughout). The mass differences with respect to the Λ_b^0 mass are also reported. This analysis uses data corresponding to an integrated luminosity of 1.0 fb^{-1} and collected in pp collisions at a center-of-mass energy of $\sqrt{s} = 7 \text{ TeV}$ with the LHCb detector in 2011.

The LHCb detector [9] is a single-arm forward spectrometer covering the pseudorapidity range $2 < \eta < 5$, designed for the study of particles containing b or c quarks. The detector includes a high precision tracking system consisting of a silicon-strip vertex detector surrounding the pp interaction region, a large-area silicon-strip detector located upstream of a dipole magnet with a bending power of about 4 T m , and three stations of silicon-strip detectors and straw drift tubes placed downstream. The combined tracking system has a momentum resolution $\Delta p/p$ that varies from 0.4% at $5 \text{ GeV}/c$ to 0.6% at $100 \text{ GeV}/c$, and an impact parameter resolution of $20 \mu\text{m}$ for tracks with high transverse momentum. Charged hadrons are identified using two ring-imaging Cherenkov detectors. Photon, electron, and hadron candidates are identified by a calorimeter system consisting of scintillating-pad and preshower detectors, an electromagnetic calorimeter, and a hadronic calorimeter. Muons are identified by a system composed of alternating layers of iron and multiwire proportional chambers. The trigger [10] consists of a hardware stage, based on information from the calorimeter and muon systems, followed by a software stage which applies a full event reconstruction.

Precision mass measurements require the momenta of the final state particles to be determined accurately. Therefore, an important feature of this analysis is the calibration of the tracker response. This accounts for imperfect knowledge of the magnetic field and tracker alignment [11]. In order to reduce these dominant contributions to the systematic uncertainty, a two-step momentum calibration

*Full author list given at the end of the article.

Published by the American Physical Society under the terms of the [Creative Commons Attribution 3.0 License](https://creativecommons.org/licenses/by/3.0/). Further distribution of this work must maintain attribution to the author(s) and the published article's title, journal citation, and DOI.

procedure is applied. First, inclusive $J/\psi \rightarrow \mu^+ \mu^-$ decays are used to account for the changes in the relative momentum scale between different data taking periods. Second, the absolute scale is derived from $B^+ \rightarrow J/\psi K^+$ decays, taking the known masses [2] as references. In this procedure, the use of a J/ψ mass constraint allows the momentum scale to be determined as a function of the K^+ track kinematics. The resulting calibration is checked with the fully reconstructed decays listed in Fig. 1. For each mode the mass distribution is modeled taking into account the effect of QED radiative corrections, resolution and background, and the mean mass value is determined. Following the procedure of Ref. [11], the deviation of the measured mass from the expected value is converted into an estimate of an average momentum scale bias independent of time and track kinematics. The bias is referred to as α , which is defined such that the measured mass becomes equal to the expected value if all particle momenta are multiplied by $1 - \alpha$. By definition, one expects $\alpha = 0$ to a good precision for the $B^+ \rightarrow J/\psi K^+$ calibration mode. Figure 1 shows the resulting values of α . The nominal mass measurements are performed with $\alpha = 0$ and the largest value of $|\alpha|$ amongst the considered modes, 0.3×10^{-3} , is conservatively taken as the systematic uncertainty on the calibrated momentum scale. This uncertainty is somewhat larger than the 0.2×10^{-3} achieved with the 2010 data [11], due to changes in the alignment of the tracking devices.

As a further check, the B^0 mass has been studied with the $B^0 \rightarrow J/\psi K_S^0$ mode, which has the same topology as $\Lambda_b^0 \rightarrow J/\psi \Lambda$. The values obtained for different run conditions and for K_S^0 decays outside or inside the vertex

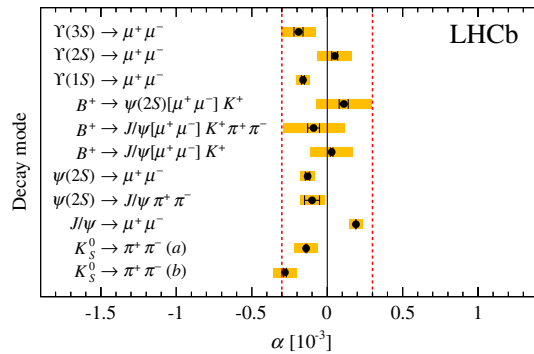


FIG. 1 (color online). Average momentum scale bias α determined from the reconstructed mass of various decay modes after the momentum calibration procedure. The K_S^0 decays are divided into two categories according to whether both daughter tracks (a) have hits or (b) do not have hits in the vertex detector. The black error bars represent the statistical uncertainty while the (yellow) filled areas also include contributions to the systematic uncertainty from the fitting procedure, the effect of QED radiative corrections, and the uncertainty on the mass of the decaying meson [2]. The (red) dashed lines show the assigned uncertainty of $\pm 0.3 \times 10^{-3}$ on the momentum scale.

detector are all in good agreement with the B^0 world average mass [2].

The decays reconstructed in this analysis, $\Lambda_b^0 \rightarrow J/\psi \Lambda$, $\Xi_b^- \rightarrow J/\psi \Xi^-$, and $\Omega_b^- \rightarrow J/\psi \Omega^-$, followed by $J/\psi \rightarrow \mu^+ \mu^-$, $\Lambda \rightarrow p \pi^-$, $\Xi^- \rightarrow \Lambda \pi^-$, and $\Omega^- \rightarrow \Lambda K^-$, are characterized by the long-lived particles in the decay chain. The lifetime of weakly decaying b baryons is ~ 1.5 ps and their decay vertex is separated from the primary pp interaction vertex by ~ 6 mm on average. The J/ψ candidates are reconstructed from pairs of oppositely charged tracks, originating from the secondary vertex, that have hits in the muon detector. In the $\Xi_b^- (\Omega_b^-)$ decay chain the long-lived $\Xi^- (\Omega^-)$ decays into a Λ and a charged pion (kaon) at a tertiary vertex and the Λ decays at a quaternary vertex. Since $\sim 90\%$ of the decays are not fully contained in the vertex detector, tracks that have no hits in the vertex detector are also considered in the reconstruction of the tertiary and quaternary vertices.

The selections of Ξ_b^- and Ω_b^- candidates are identical apart from the choice of the Ξ^- , Ξ_b^- , Ω^- , Ω_b^- invariant mass ranges and particle identification requirements on the pion (kaon) from the $\Xi^- (\Omega^-)$ vertex. The Λ_b^0 selection is slightly different, owing to the different topology.

The J/ψ candidates are required to satisfy $|M_{\mu\mu} - M_{J/\psi}| < 4.2\sigma$ where $M_{\mu\mu}$ is the reconstructed dimuon mass, $M_{J/\psi}$ the J/ψ mass [2], and σ the estimated event-by-event uncertainty on $M_{\mu\mu}$ (typically $10 \text{ MeV}/c^2$). The invariant mass windows for the Λ , Ξ^- and Ω^- candidates are $\pm 6 \text{ MeV}/c^2$, $\pm 11 \text{ MeV}/c^2$ and $\pm 11 \text{ MeV}/c^2$ around the expected masses [2], respectively. Particle identification requirements are applied to the kaon from the Ω^- candidate and the proton from the Λ decay to improve the purity of the selected daughter particles, but none is placed on the pion from the Ξ^- candidate. In addition, the hyperon decay vertices are required to be downstream of the b -hadron decay vertex.

The Λ_b^0 , Ξ_b^- , and Ω_b^- mass resolutions are improved by performing a fit of the decay topology and vertices [12] while constraining the masses of the J/ψ , Λ , Ξ^- , and Ω^- hadrons to have their known values [2], the final-state and intermediate long-lived particles to originate from common vertices according to the decay chain, and the b baryon to originate from the primary vertex. Three additional selection variables are considered: the χ^2 per degree of freedom ($\chi^2/\text{d.o.f.}$) from the fit, the reconstructed decay time and the χ_{IP}^2 , defined as the difference in the χ^2 of the primary vertex fit with and without the b -baryon candidate. In the case of the Ξ_b^- candidates, the selection requirements for these variables are chosen to maximize the expected significance of the Ξ_b^- signal; the same selection is used for the Ω_b^- candidates. To determine the significance for a set of selection criteria the background yield is estimated from the yield of Ξ_b^- candidates found in mass sidebands in the ranges $5600\text{--}5700 \text{ MeV}/c^2$ and $5900\text{--}6100 \text{ MeV}/c^2$. The expected signal yield is

estimated using the product of the world average hadronization fraction for $b \rightarrow \Xi_b^-$ and branching fractions for $\Xi_b^- \rightarrow J/\psi \Xi^-$ and subsequent daughter particle decays [2], the $b\bar{b}$ production cross section in the LHCb acceptance [13] and the selection efficiencies obtained from simulation. The selection criteria giving the highest expected signal significance correspond to a decay time greater than 0.25 ps, a $\chi^2/\text{d.o.f.}$ smaller than 4 and a χ^2_{IP} smaller than 16. Amongst these, the decay time requirement is the most powerful given the high level of background close to the interaction point. In the case of the Λ_b^0 candidates, the decay time is required to be greater than 0.3 ps and the $\chi^2/\text{d.o.f.}$ smaller than 5 (no requirement on the χ^2_{IP} is made). The possibility of a cross-feed background between Ξ_b^- and Ω_b^- is investigated using simulation and found to be negligible in comparison with the combinatorial background.

The invariant mass distributions of the selected Λ_b^0 , Ξ_b^- , and Ω_b^- candidates are shown in Fig. 2. The Λ_b^0 , Ξ_b^- , Ω_b^- masses are measured by performing an unbinned extended maximum likelihood fit in the ranges 5500–5750, 5600–6000, 5800–6300 MeV/ c^2 , respectively. The signal component is described with a single Gaussian function (or the sum of two Gaussian functions with common mean in the case of the Λ_b^0 baryon) and the background is modeled with an exponential function. The widths of the Λ_b^0 and Ξ_b^- signals are left unconstrained in the fit. Because of the low expected yield for the Ω_b^- signal, the width of the Gaussian function describing the Ω_b^- signal is fixed to the measured Ξ_b^- signal width multiplied by the ratio of Ω_b^- and Ξ_b^- widths from the simulation (8.2 MeV/ c^2 for Ω_b^- and 8.9 MeV/ c^2 for Ξ_b^-). The fit results are given in Table I.

The statistical significance of the Ω_b^- signal is determined using simulated pseudoexperiments with background only. We determine the probability that, anywhere in the mass range between 5800 and 6300 MeV/ c^2 , a peak appears with the expected width and a yield at least as large as that observed in the data. This probability corresponds to 6 standard deviations, which we interpret as the statistical significance of the Ω_b^- signal.

The systematic uncertainties are evaluated by repeating the complete analysis (including the track fit and the momentum scale calibration when needed), varying in turn within its uncertainty each parameter to which the mass determination is sensitive. The observed changes in the central values of the fitted masses relative to the nominal results are then assigned as systematic uncertainties and summed in quadrature (see Table II).

The dominant systematic uncertainty is due to the momentum scale calibration described previously, which is assigned an uncertainty of $\pm 0.3 \times 10^{-3}$. Most of the uncertainty related to the momentum scale is removed in the measurements of the mass differences.

The uncertainty on the amount of material assumed in the track reconstruction for the energy loss (dE/dx)

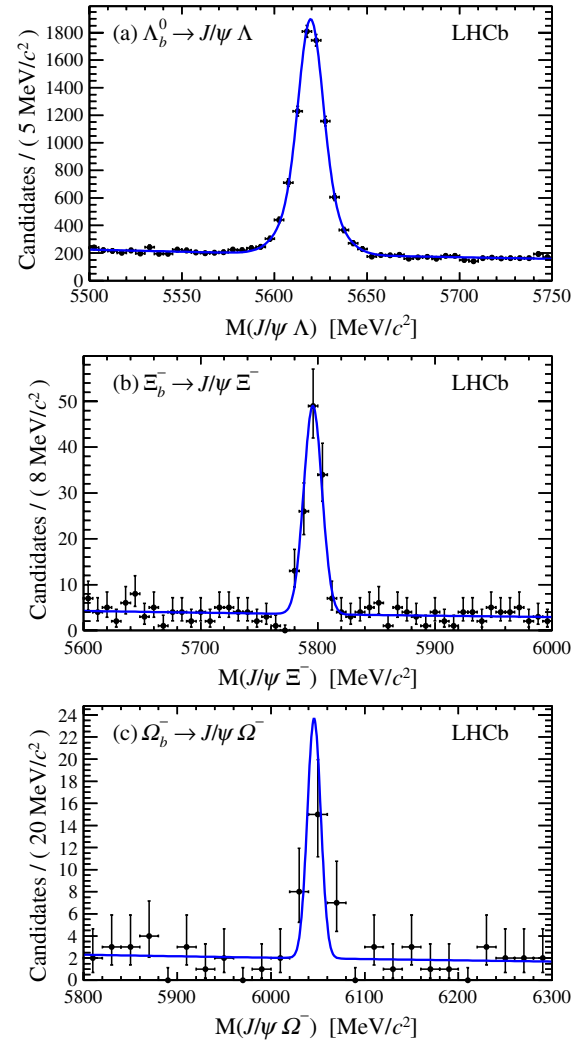


FIG. 2 (color online). Invariant mass distribution for (a) $\Lambda_b^0 \rightarrow J/\psi \Lambda$, (b) $\Xi_b^- \rightarrow J/\psi \Xi^-$, and (c) $\Omega_b^- \rightarrow J/\psi \Omega^-$ candidates. The results of the unbinned maximum likelihood fits are shown with solid lines.

correction has been found to be small [11]. It translates into an uncertainty on the Λ_b^0 mass of 0.09 MeV/ c^2 , which we apply to all masses.

The b -baryon invariant masses are computed assuming the central values of the Λ , Ξ^- , and Ω^- world-average

TABLE I. Results of the fits to the invariant mass distributions. The quoted uncertainties are statistical. The Λ_b^0 signal is described by a double Gaussian function with widths σ_1 and σ_2 ; the fraction of the yield described by the first component is 0.58 ± 0.11 .

| | Signal yield | Mass (MeV/ c^2) | Width(s) (MeV/ c^2) |
|---------------|----------------|--------------------|---|
| Λ_b^0 | 6870 ± 110 | 5619.53 ± 0.13 | $\sigma_1 = 6.4 \pm 0.5$ $\sigma_2 = 12.5 \pm 1.3$ |
| Ξ_b^- | 111 ± 12 | 5795.8 ± 0.9 | 7.8 ± 0.7 |
| Ω_b^- | 19 ± 5 | 6046.0 ± 2.2 | 7.2 (fixed) |

TABLE II. Systematic uncertainties (in MeV/c^2) on the mass measurements and their differences. The total systematic uncertainty is obtained from adding all uncertainties in quadrature.

| Source | Λ_b^0 | Ξ_b^- | Ω_b^- | $\Xi_b^- - \Lambda_b^0$ | $\Omega_b^- - \Lambda_b^0$ |
|--------------------|---------------|-----------|--------------|-------------------------|----------------------------|
| Momentum scale | 0.43 | 0.43 | 0.31 | 0.01 | 0.12 |
| dE/dx correction | 0.09 | 0.09 | 0.09 | 0.01 | 0.01 |
| Hyperon mass | 0.01 | 0.07 | 0.25 | 0.07 | 0.25 |
| Signal model | 0.07 | 0.01 | 0.24 | 0.07 | 0.25 |
| Background model | 0.01 | 0.01 | 0.02 | 0.01 | 0.02 |
| Total | 0.45 | 0.45 | 0.47 | 0.10 | 0.37 |

masses [2]. The uncertainties on these values are propagated as systematic uncertainties.

Two alternative fits for the Λ_b^0 signal are performed: a first fit where the candidates are split into two categories depending on whether the daughter tracks have vertex detector information or not, each category being described with a single Gaussian function where the two Gaussian functions have a common mean, and a second fit using the sum of two Crystal Ball functions [14] with common peak value and otherwise unconstrained parameters. The second fit allows us to take into account possible QED radiative corrections.

The Ξ_b^- mass fit is repeated using as an alternative model either the sum of two Gaussian functions with a common mean, or a single Crystal Ball function. In the Ω_b^- mass fit, the fixed Gaussian width is varied within both the uncertainty of the fitted Ξ_b^- width and the uncertainty of the width ratio from simulation.

An alternative background model assuming a linear shape leads to negligible changes. We also repeat the Ξ_b^- and Ω_b^- mass fits in a restricted mass range of $5650\text{--}5950\text{ MeV}/c^2$ and $5900\text{--}6200\text{ MeV}/c^2$, respectively.

In summary, the Λ_b^0 , Ξ_b^- and Ω_b^- baryons are observed in the $\Lambda_b^0 \rightarrow J/\psi \Lambda$, $\Xi_b^- \rightarrow J/\psi \Xi^-$ and $\Omega_b^- \rightarrow J/\psi \Omega^-$ decay modes using 1.0 fb^{-1} of pp collisions collected in 2011 at a center-of-mass energy of $\sqrt{s} = 7\text{ TeV}$. The statistical significance of the observed $\Omega_b^- \rightarrow J/\psi \Omega^-$ signal is 6 standard deviations. The masses of the b baryons are measured to be

$$M(\Lambda_b^0) = 5619.53 \pm 0.13 \pm 0.45\text{ MeV}/c^2,$$

$$M(\Xi_b^-) = 5795.8 \pm 0.9 \pm 0.4\text{ MeV}/c^2,$$

$$M(\Omega_b^-) = 6046.0 \pm 2.2 \pm 0.5\text{ MeV}/c^2,$$

where the first (second) quoted uncertainty is statistical (systematic). The dominant systematic uncertainty, due to the knowledge of the momentum scale, partially cancels in mass differences. We obtain

$$M(\Xi_b^-) - M(\Lambda_b^0) = 176.2 \pm 0.9 \pm 0.1\text{ MeV}/c^2,$$

$$M(\Omega_b^-) - M(\Lambda_b^0) = 426.4 \pm 2.2 \pm 0.4\text{ MeV}/c^2.$$

A measurement of the Λ_b^0 mass based on the 2010 data sample, $M(\Lambda_b^0) = 5619.19 \pm 0.70 \pm 0.30\text{ MeV}/c^2$,

TABLE III. Comparison of the b -baryon mass measurements using the full 2011 data sample with the single most precise results from the ATLAS [15], CDF [5,16], and D0 [4,6] collaborations, and with the PDG averages [2]. The PDG averages contain the results from CDF and D0 as well as the Λ_b^0 measurement from LHCb performed with the 2010 data sample. The quoted errors include statistical and systematic uncertainties. All values are in MeV/c^2 .

| | $M(\Lambda_b^0)$ | $M(\Xi_b^-)$ | $M(\Omega_b^-)$ |
|-------|------------------|------------------|------------------|
| ATLAS | 5619.7 ± 1.3 | ... | ... |
| CDF | 5619.7 ± 1.7 | 5790.9 ± 2.7 | 6054.4 ± 6.9 |
| D0 | ... | 5774 ± 19 | 6165 ± 16 |
| PDG | 5619.4 ± 0.7 | 5791.1 ± 2.2 | 6071 ± 40 |
| LHCb | 5619.5 ± 0.5 | 5795.8 ± 1.0 | 6046.0 ± 2.3 |

has been previously reported by LHCb [11]. Since the new alignment and momentum calibration procedures differ from those applied in the previous study, a possible correlation between the systematic uncertainties related to the momentum scale can be neglected. Considering that the only correlated systematic uncertainties are those due to energy loss correction and mass fitting, the weighted average of the two Λ_b^0 mass measurements that minimizes the total uncertainty is

$$M(\Lambda_b^0) = 5619.44 \pm 0.13 \pm 0.38\text{ MeV}/c^2.$$

These Λ_b^0 , Ξ_b^- , and Ω_b^- mass measurements are the most precise to date. They are compared in Table III with the single most precise measurements from ATLAS, CDF, and D0, and with the current world averages [2]. The Λ_b^0 and Ξ_b^- results are in agreement with previous measurements. The Ω_b^- result is in agreement with the CDF measurement [5], but in disagreement with the D0 measurement [4].

We express our gratitude to our colleagues in the CERN accelerator departments for the excellent performance of the LHC. We thank the technical and administrative staff at the LHCb institutes. We acknowledge support from CERN and from the national agencies: CAPES, CNPq, FAPERJ and FINEP (Brazil); NSFC (China); CNRS/IN2P3 and Region Auvergne (France); BMBF, DFG, HGF and MPG (Germany); SFI (Ireland); INFN (Italy); FOM and NWO (The Netherlands); SCSR (Poland); ANCS/IFA (Romania); MinES, Rosatom, RFBR and NRC ‘‘Kurchatov Institute’’ (Russia); MinECo, XuntaGal and GENCAT (Spain); SNSF and SER (Switzerland); NAS Ukraine (Ukraine); STFC (United Kingdom); NSF (USA). We also acknowledge the support received from the ERC under FP7. The Tier1 computing centers are supported by IN2P3 (France), KIT and BMBF (Germany), INFN (Italy), NWO and SURF (The Netherlands), PIC (Spain), GridPP (United Kingdom). We are thankful for the computing resources put at our disposal by Yandex LLC (Russia), as well as to the communities behind the multiple open source software packages that we depend on.

- [1] C. Amsler, T. Degrand, and B. Krusche, Quark Model, published in Ref. [2].
- [2] J. Beringer *et al.* (Particle Data Group), *Phys. Rev. D* **86**, 010001 (2012).
- [3] M. Karliner, B. Keren-Zur, H. Lipkin, and J. Rosner, *Ann. Phys. (Amsterdam)* **324**, 2 (2009); J.P. Day, W. Plessas, and K.-S. Choi, [arXiv:1205.6918](https://arxiv.org/abs/1205.6918); X. Liu, H.-X. Chen, Y.-R. Liu, A. Hosaka, and S.-L. Zhu, *Phys. Rev. D* **77**, 014031 (2008); J.-R. Zhang and M.-Q. Huang, *Phys. Rev. D* **78**, 094015 (2008); E.E. Jenkins, *Phys. Rev. D* **77**, 034012 (2008); R. Roncaglia, D. Lichtenberg, and E. Predazzi, *Phys. Rev. D* **52**, 1722 (1995); R. Lewis and R. Woloshyn, *Phys. Rev. D* **79**, 014502 (2009); D. Ebert, R. Faustov, and V. Galkin, *Phys. Rev. D* **72**, 034026 (2005).
- [4] V. Abazov *et al.* (D0 Collaboration), *Phys. Rev. Lett.* **101**, 232002 (2008).
- [5] T. Aaltonen *et al.* (CDF Collaboration), *Phys. Rev. D* **80**, 072003 (2009).
- [6] V. Abazov *et al.* (D0 Collaboration), *Phys. Rev. Lett.* **99**, 052001 (2007).
- [7] T. Aaltonen *et al.* (CDF Collaboration), *Phys. Rev. Lett.* **99**, 052002 (2007).
- [8] T. Aaltonen *et al.* (CDF Collaboration), *Phys. Rev. Lett.* **107**, 102001 (2011).
- [9] A.A. Alves, Jr. *et al.* (LHCb Collaboration), *JINST* **3**, S08005 (2008).
- [10] R. Aaij *et al.*, [arXiv:1211.3055](https://arxiv.org/abs/1211.3055).
- [11] R. Aaij *et al.* (LHCb Collaboration), *Phys. Lett. B* **708**, 241 (2012).
- [12] W.D. Hulsbergen, *Nucl. Instrum. Methods Phys. Res., Sect. A* **552**, 566 (2005).
- [13] R. Aaij *et al.* (LHCb Collaboration), *Phys. Lett. B* **694**, 209 (2010).
- [14] T. Skwarnicki, Ph.D. thesis, Institute of Nuclear Physics, Krakow, 1986.
- [15] G. Aad *et al.* (ATLAS Collaboration), [arXiv:1207.2284](https://arxiv.org/abs/1207.2284).
- [16] D. Acosta *et al.* (CDF Collaboration), *Phys. Rev. Lett.* **96**, 202001 (2006).

R. Aaij,³⁸ C. Abellan Beteta,^{33,a} A. Adametz,¹¹ B. Adeva,³⁴ M. Adinolfi,⁴³ C. Adrover,⁶ A. Affolder,⁴⁹ Z. Ajaltouni,⁵ J. Albrecht,⁹ F. Alessio,³⁵ M. Alexander,⁴⁸ S. Ali,³⁸ G. Alkhazov,²⁷ P. Alvarez Cartelle,³⁴ A. A. Alves, Jr.,^{22,35} S. Amato,² Y. Amhis,⁷ L. Anderlini,^{17,b} J. Anderson,³⁷ R. Andreassen,⁵⁷ R. B. Appleby,⁵¹ O. Aquines Gutierrez,¹⁰ F. Archilli,¹⁸ A. Artamonov,³² M. Artuso,⁵³ E. Aslanides,⁶ G. Auriemma,^{22,c} S. Bachmann,¹¹ J. J. Back,⁴⁵ C. Baesso,⁵⁴ V. Balagura,²⁸ W. Baldini,¹⁶ R. J. Barlow,⁵¹ C. Barschel,³⁵ S. Barsuk,⁷ W. Barter,⁴⁴ Th. Bauer,³⁸ A. Bay,³⁶ J. Beddow,⁴⁸ I. Bediaga,¹ S. Belogurov,²⁸ K. Belous,³² I. Belyaev,²⁸ E. Ben-Haim,⁸ M. Benayoun,⁸ G. Bencivenni,¹⁸ S. Benson,⁴⁷ J. Benton,⁴³ A. Berezhnoy,²⁹ R. Bernet,³⁷ M.-O. Bettler,⁴⁴ M. van Beuzekom,³⁸ A. Bien,¹¹ S. Bifani,¹² T. Bird,⁵¹ A. Bizzeti,^{17,d} P. M. Bjørnstad,⁵¹ T. Blake,³⁵ F. Blanc,³⁶ C. Blanks,⁵⁰ J. Blouw,¹¹ S. Blusk,⁵³ A. Bobrov,³¹ V. Bocci,²² A. Bondar,³¹ N. Bondar,²⁷ W. Bonivento,¹⁵ S. Borghi,⁵¹ A. Borgia,⁵³ T. J. V. Bowcock,⁴⁹ E. Bowen,³⁷ C. Bozzi,¹⁶ T. Brambach,⁹ J. van den Brand,³⁹ J. Bressieux,³⁶ D. Brett,⁵¹ M. Britsch,¹⁰ T. Britton,⁵³ N. H. Brook,⁴³ H. Brown,⁴⁹ I. Burducea,²⁶ A. Bursche,³⁷ J. Buytaert,³⁵ S. Cadeddu,¹⁵ O. Callot,⁷ M. Calvi,^{20,e} M. Calvo Gomez,^{33,a} A. Camboni,³³ P. Campana,^{18,35} A. Carbone,^{14,f} G. Carboni,^{21,g} R. Cardinale,^{19,h} A. Cardini,¹⁵ H. Carranza-Mejia,⁴⁷ L. Carson,⁵⁰ K. Carvalho Akiba,² G. Casse,⁴⁹ M. Cattaneo,³⁵ Ch. Cauet,⁹ M. Charles,⁵² Ph. Charpentier,³⁵ P. Chen,^{3,36} N. Chiapolini,³⁷ M. Chrzasczcz,²³ K. Ciba,³⁵ X. Cid Vidal,³⁴ G. Ciezarek,⁵⁰ P. E. L. Clarke,⁴⁷ M. Clemencic,³⁵ H. V. Cliff,⁴⁴ J. Closier,³⁵ C. Coca,²⁶ V. Coco,³⁸ J. Cogan,⁶ E. Cogneras,⁵ P. Collins,³⁵ A. Comerma-Montells,³³ A. Contu,^{15,52} A. Cook,⁴³ M. Coombes,⁴³ S. Coquereau,⁸ G. Corti,³⁵ B. Couturier,³⁵ G. A. Cowan,³⁶ D. Craik,⁴⁵ S. Cunliffe,⁵⁰ R. Currie,⁴⁷ C. D'Ambrosio,³⁵ P. David,⁸ P. N. Y. David,³⁸ I. De Bonis,⁴ K. De Bruyn,³⁸ S. De Capua,⁵¹ M. De Cian,³⁷ J. M. De Miranda,¹ L. De Paula,² W. De Silva,⁵⁷ P. De Simone,¹⁸ D. Decamp,⁴ M. Deckenhoff,⁹ H. Degaudenzi,^{36,35} L. Del Buono,⁸ C. Deplano,¹⁵ D. Derkach,¹⁴ O. Deschamps,⁵ F. Dettori,³⁹ A. Di Canto,¹¹ J. Dickens,⁴⁴ H. Dijkstra,³⁵ M. Dogaru,²⁶ F. Domingo Bonal,^{33,a} S. Donleavy,⁴⁹ F. Dordei,¹¹ A. Dosil Suárez,³⁴ D. Dossett,⁴⁵ A. Dovbnya,⁴⁰ F. Dupertuis,³⁶ R. Dzhelyadin,³² A. Dziurda,²³ A. Dzyuba,²⁷ S. Easo,^{46,35} U. Egede,⁵⁰ V. Egorychev,²⁸ S. Eidelman,³¹ D. van Eijk,³⁸ S. Eisenhardt,⁴⁷ U. Eitschberger,⁹ R. Ekelhof,⁹ L. Eklund,⁴⁸ I. El Rifai,⁵ Ch. Elsasser,³⁷ D. Elsby,⁴² A. Falabella,^{14,i} C. Färber,¹¹ G. Fardell,⁴⁷ C. Farinelli,³⁸ S. Farry,¹² V. Fave,³⁶ D. Ferguson,⁴⁷ V. Fernandez Albor,³⁴ F. Ferreira Rodrigues,¹ M. Ferro-Luzzi,³⁵ S. Filippov,³⁰ C. Fitzpatrick,³⁵ M. Fontana,¹⁰ F. Fontanelli,^{19,h} R. Forty,³⁵ O. Francisco,² M. Frank,³⁵ C. Frei,³⁵ M. Frosini,^{17,b} S. Furcas,²⁰ E. Furfaro,²¹ A. Gallas Torreira,³⁴ D. Galli,^{14,f} M. Gandelman,² P. Gandini,⁵² Y. Gao,³ J. Garofoli,⁵³ P. Garosi,⁵¹ J. Garra Tico,⁴⁴ L. Garrido,³³ C. Gaspar,³⁵ R. Gauld,⁵² E. Gersabeck,¹¹ M. Gersabeck,⁵¹ T. Gershon,^{45,35} Ph. Ghez,⁴ V. Gibson,⁴⁴ V. V. Gligorov,³⁵ C. Göbel,⁵⁴ D. Golubkov,²⁸ A. Golutvin,^{50,28,35} A. Gomes,² H. Gordon,⁵² M. Grabalosa Gándara,⁵ R. Graciani Diaz,³³ L. A. Granado Cardoso,³⁵ E. Graugés,³³ G. Graziani,¹⁷ A. Grecu,²⁶ E. Greening,⁵² S. Gregson,⁴⁴ O. Grünberg,⁵⁵ B. Gui,⁵³ E. Gushchin,³⁰ Yu. Guz,³² T. Gys,³⁵ C. Hadjivasiliou,⁵³ G. Haefeli,³⁶ C. Haen,³⁵ S. C. Haines,⁴⁴ S. Hall,⁵⁰ T. Hampson,⁴³ S. Hansmann-Menzemer,¹¹ N. Harnew,⁵² S. T. Harnew,⁴³ J. Harrison,⁵¹ P. F. Harrison,⁴⁵

T. Hartmann,⁵⁵ J. He,⁷ V. Heijne,³⁸ K. Hennessy,⁴⁹ P. Henrard,⁵ J. A. Hernando Morata,³⁴ E. van Herwijnen,³⁵ E. Hicks,⁴⁹ D. Hill,⁵² M. Hoballah,⁵ C. Hombach,⁵¹ P. Hopchev,⁴ W. Hulsbergen,³⁸ P. Hunt,⁵² T. Huse,⁴⁹ N. Hussain,⁵² D. Hutchcroft,⁴⁹ D. Hynds,⁴⁸ V. Iakovenko,⁴¹ P. Ilten,¹² R. Jacobsson,³⁵ A. Jaeger,¹¹ E. Jans,³⁸ F. Jansen,³⁸ P. Jaton,³⁶ F. Jing,³ M. John,⁵² D. Johnson,⁵² C. R. Jones,⁴⁴ B. Jost,³⁵ M. Kabbalo,⁹ S. Kandybei,⁴⁰ M. Karacson,³⁵ T. M. Karbach,³⁵ I. R. Kenyon,⁴² U. Kerzel,³⁵ T. Ketel,³⁹ A. Keune,³⁶ B. Khanji,²⁰ O. Kochebina,⁷ I. Komarov,^{36,29} R. F. Koopman,³⁹ P. Koppenburg,³⁸ M. Korolev,²⁹ A. Kozlinskiy,³⁸ L. Kravchuk,³⁰ K. Kreplin,¹¹ M. Kreps,⁴⁵ G. Krocker,¹¹ P. Krokovny,³¹ F. Kruse,⁹ M. Kucharczyk,^{20,23,e} V. Kudryavtsev,³¹ T. Kvaratskheliya,^{28,35} V. N. La Thi,³⁶ D. Lacarrere,³⁵ G. Lafferty,⁵¹ A. Lai,¹⁵ D. Lambert,⁴⁷ R. W. Lambert,³⁹ E. Lanciotti,³⁵ G. Lanfranchi,^{18,35} C. Langenbruch,³⁵ T. Latham,⁴⁵ C. Lazzeroni,⁴² R. Le Gac,⁶ J. van Leerdam,³⁸ J.-P. Lees,⁴ R. Lefèvre,⁵ A. Leflat,^{29,35} J. Lefrançois,⁷ O. Leroy,⁶ Y. Li,³ L. Li Gioi,⁵ M. Liles,⁴⁹ R. Lindner,³⁵ C. Linn,¹¹ B. Liu,³ G. Liu,³⁵ J. von Loeben,²⁰ J. H. Lopes,² E. Lopez Asamar,³³ N. Lopez-March,³⁶ H. Lu,³ J. Luisier,³⁶ H. Luo,⁴⁷ F. Machefert,⁷ I. V. Machikhiliyan,^{4,28} F. Maciuc,²⁶ O. Maev,^{27,35} S. Malde,⁵² G. Manca,^{15,j} G. Mancinelli,⁶ N. Mangiafave,⁴⁴ U. Marconi,¹⁴ R. Märki,³⁶ J. Marks,¹¹ G. Martellotti,²² A. Martens,⁸ L. Martin,⁵² A. Martín Sánchez,⁷ M. Martinelli,³⁸ D. Martinez Santos,³⁹ D. Martins Tostes,² A. Massafferri,¹ R. Matev,³⁵ Z. Mathe,³⁵ C. Matteuzzi,²⁰ M. Matveev,²⁷ E. Maurice,⁶ A. Mazurov,^{16,30,35,i} J. McCarthy,⁴² R. McNulty,¹² B. Meadows,^{57,52} F. Meier,⁹ M. Meissner,¹¹ M. Merk,³⁸ D. A. Milanes,⁸ M.-N. Minard,⁴ J. Molina Rodriguez,⁵⁴ S. Monteil,⁵ D. Moran,⁵¹ P. Morawski,²³ R. Mountain,⁵³ I. Mous,³⁸ F. Muheim,⁴⁷ K. Müller,³⁷ R. Muresan,²⁶ B. Muryn,²⁴ B. Muster,³⁶ P. Naik,⁴³ T. Nakada,³⁶ R. Nandakumar,⁴⁶ I. Nasteva,¹ M. Needham,⁴⁷ N. Neufeld,³⁵ A. D. Nguyen,³⁶ T. D. Nguyen,³⁶ C. Nguyen-Mau,^{36,k} M. Nicol,⁷ V. Niess,⁵ R. Niet,⁹ N. Nikitin,²⁹ T. Nikodem,¹¹ S. Nisar,⁵⁶ A. Nomerotski,⁵² A. Novoselov,³² A. Oblakowska-Mucha,²⁴ V. Obraztsov,³² S. Oggero,³⁸ S. Ogilvy,⁴⁸ O. Okhrimenko,⁴¹ R. Oldeman,^{15,35,j} M. Orlandea,²⁶ J. M. Otorola Goicochea,² P. Owen,⁵⁰ B. K. Pal,⁵³ A. Palano,^{13,l} M. Palutan,¹⁸ J. Panman,³⁵ A. Papanestis,⁴⁶ M. Pappagallo,⁴⁸ C. Parkes,⁵¹ C. J. Parkinson,⁵⁰ G. Passaleva,¹⁷ G. D. Patel,⁴⁹ M. Patel,⁵⁰ G. N. Patrick,⁴⁶ C. Patrignani,^{19,h} C. Pavel-Nicorescu,²⁶ A. Pazos Alvarez,³⁴ A. Pellegrino,³⁸ G. Penso,^{22,m} M. Pepe Altarelli,³⁵ S. Perazzini,^{14,f} D. L. Perego,^{20,e} E. Perez Trigo,³⁴ A. Pérez-Calero Yzquierdo,³³ P. Perret,⁵ M. Perrin-Terrin,⁶ G. Pessina,²⁰ K. Petridis,⁵⁰ A. Petrolini,^{19,h} A. Phan,⁵³ E. Picatoste Olloqui,³³ B. Pietrzyk,⁴ T. Pilarš,⁴⁵ D. Pinci,²² S. Playfer,⁴⁷ M. Plo Casasus,³⁴ F. Polci,⁸ G. Polok,²³ A. Poluektov,^{45,31} E. Polycarpo,² D. Popov,¹⁰ B. Popovici,²⁶ C. Potterat,³³ A. Powell,⁵² J. Prisciandaro,³⁶ V. Pugatch,⁴¹ A. Puig Navarro,³⁶ W. Qian,⁴ J. H. Rademacker,⁴³ B. Rakotomiamanana,³⁶ M. S. Rangel,² I. Raniuk,⁴⁰ N. Rauschmayr,³⁵ G. Raven,³⁹ S. Redford,⁵² M. M. Reid,⁴⁵ A. C. dos Reis,¹ S. Ricciardi,⁴⁶ A. Richards,⁵⁰ K. Rinnert,⁴⁹ V. Rives Molina,³³ D. A. Roa Romero,⁵ P. Robbe,⁷ E. Rodrigues,⁵¹ P. Rodriguez Perez,³⁴ G. J. Rogers,⁴⁴ S. Roiser,³⁵ V. Romanovsky,³² A. Romero Vidal,³⁴ J. Rouvinet,³⁶ T. Ruf,³⁵ H. Ruiz,³³ G. Sabatino,^{22,g} J. J. Saborido Silva,³⁴ N. Sagidova,²⁷ P. Sail,⁴⁸ B. Saitta,^{15,j} C. Salzmann,³⁷ B. Sanmartin Sedes,³⁴ M. Sannino,^{19,h} R. Santacesaria,²² C. Santamarina Rios,³⁴ E. Santovetti,^{21,g} M. Sapunov,⁶ A. Sarti,^{18,m} C. Satriano,^{22,c} A. Satta,²¹ M. Savrie,^{16,i} D. Savrina,^{28,29} P. Schaack,⁵⁰ M. Schiller,³⁹ H. Schindler,³⁵ S. Schleich,⁹ M. Schlupp,⁹ M. Schmelling,¹⁰ B. Schmidt,³⁵ O. Schneider,³⁶ A. Schopper,³⁵ M.-H. Schune,⁷ R. Schwemmer,³⁵ B. Sciascia,¹⁸ A. Sciubba,^{18,m} M. Seco,³⁴ A. Semennikov,²⁸ K. Senderowska,²⁴ I. Sepp,⁵⁰ N. Serra,³⁷ J. Serrano,⁶ P. Seyfert,¹¹ M. Shapkin,³² I. Shapoval,^{40,35} P. Shatalov,²⁸ Y. Shcheglov,²⁷ T. Shears,^{49,35} L. Shekhtman,³¹ O. Shevchenko,⁴⁰ V. Shevchenko,²⁸ A. Shires,⁵⁰ R. Silva Coutinho,⁴⁵ T. Skwarnicki,⁵³ N. A. Smith,⁴⁹ E. Smith,^{52,46} M. Smith,⁵¹ K. Sobczak,⁵ M. D. Sokoloff,⁵⁷ F. J. P. Soler,⁴⁸ F. Soomro,^{18,35} D. Souza,⁴³ B. Souza De Paula,² B. Spaan,⁹ A. Sparkes,⁴⁷ P. Spradlin,⁴⁸ F. Stagni,³⁵ S. Stahl,¹¹ O. Steinkamp,³⁷ S. Stoica,²⁶ S. Stone,⁵³ B. Storaci,³⁷ M. Straticiu,²⁶ U. Straumann,³⁷ V. K. Subbiah,³⁵ S. Swientek,⁹ V. Syropoulos,³⁹ M. Szczekowski,²⁵ P. Szczypka,^{36,35} T. Szumlak,²⁴ S. T'Jampens,⁴ M. Teklishyn,⁷ E. Teodoroescu,²⁶ F. Teubert,³⁵ C. Thomas,⁵² E. Thomas,³⁵ J. van Tilburg,¹¹ V. Tisserand,⁴ M. Tobin,³⁷ S. Tolk,³⁹ D. Tonelli,³⁵ S. Topp-Joergensen,⁵² N. Torr,⁵² E. Tournefier,^{4,50} S. Tourneur,³⁶ M. T. Tran,³⁶ M. Tresch,³⁷ A. Tsaregorodtsev,⁶ P. Tsopelas,³⁸ N. Tuning,³⁸ M. Ubeda Garcia,³⁵ A. Ukleja,²⁵ D. Urner,⁵¹ U. Uwer,¹¹ V. Vagnoni,¹⁴ G. Valenti,¹⁴ R. Vazquez Gomez,³³ P. Vazquez Regueiro,³⁴ S. Vecchi,¹⁶ J. J. Velthuis,⁴³ M. Veltri,^{17,n} G. Veneziano,³⁶ M. Vesterinen,³⁵ B. Viaud,⁷ D. Vieira,² X. Vilasis-Cardona,^{33,a} A. Vollhardt,³⁷ D. Volyanskyy,¹⁰ D. Voong,⁴³ A. Vorobyev,²⁷ V. Vorobyev,³¹ C. Voß,⁵⁵ H. Voss,¹⁰ R. Waldi,⁵⁵ R. Wallace,¹² S. Wandernoth,¹¹ J. Wang,⁵³ D. R. Ward,⁴⁴ N. K. Watson,⁴² A. D. Webber,⁵¹ D. Websdale,⁵⁰ M. Whitehead,⁴⁵ J. Wicht,³⁵ J. Wiechczynski,²³ D. Wiedner,¹¹ L. Wiggers,³⁸ G. Wilkinson,⁵² M. P. Williams,^{45,46} M. Williams,^{50,o} F. F. Wilson,⁴⁶ J. Wishahi,⁹ M. Witek,²³ S. A. Wotton,⁴⁴ S. Wright,⁴⁴ S. Wu,³ K. Wyllie,³⁵ Y. Xie,^{47,35} F. Xing,⁵² Z. Xing,⁵³ Z. Yang,³ R. Young,⁴⁷

X. Yuan,³ O. Yushchenko,³² M. Zangoli,¹⁴ M. Zavertyaev,^{10,p} F. Zhang,³ L. Zhang,⁵³ W. C. Zhang,¹²
Y. Zhang,³ A. Zhelezov,¹¹ L. Zhong,³ and A. Zvyagin³⁵

(LHCb Collaboration)

- ¹Centro Brasileiro de Pesquisas Físicas (CBPF), Rio de Janeiro, Brazil
²Universidade Federal do Rio de Janeiro (UFRJ), Rio de Janeiro, Brazil
³Center for High Energy Physics, Tsinghua University, Beijing, China
⁴LAPP, Université de Savoie, CNRS/IN2P3, Annecy-Le-Vieux, France
⁵Clermont Université, Université Blaise Pascal, CNRS/IN2P3, LPC, Clermont-Ferrand, France
⁶CPPM, Aix-Marseille Université, CNRS/IN2P3, Marseille, France
⁷LAL, Université Paris-Sud, CNRS/IN2P3, Orsay, France
⁸LPNHE, Université Pierre et Marie Curie, Université Paris Diderot, CNRS/IN2P3, Paris, France
⁹Fakultät Physik, Technische Universität Dortmund, Dortmund, Germany
¹⁰Max-Planck-Institut für Kernphysik (MPIK), Heidelberg, Germany
¹¹Physikalisches Institut, Ruprecht-Karls-Universität Heidelberg, Heidelberg, Germany
¹²School of Physics, University College Dublin, Dublin, Ireland
¹³Sezione INFN di Bari, Bari, Italy
¹⁴Sezione INFN di Bologna, Bologna, Italy
¹⁵Sezione INFN di Cagliari, Cagliari, Italy
¹⁶Sezione INFN di Ferrara, Ferrara, Italy
¹⁷Sezione INFN di Firenze, Firenze, Italy
¹⁸Laboratori Nazionali dell'INFN di Frascati, Frascati, Italy
¹⁹Sezione INFN di Genova, Genova, Italy
²⁰Sezione INFN di Milano Bicocca, Milano, Italy
²¹Sezione INFN di Roma Tor Vergata, Roma, Italy
²²Sezione INFN di Roma La Sapienza, Roma, Italy
²³Henryk Niewodniczanski Institute of Nuclear Physics Polish Academy of Sciences, Kraków, Poland
²⁴AGH University of Science and Technology, Kraków, Poland
²⁵National Center for Nuclear Research (NCBJ), Warsaw, Poland
²⁶Horia Hulubei National Institute of Physics and Nuclear Engineering, Bucharest-Magurele, Romania
²⁷Petersburg Nuclear Physics Institute (PNPI), Gatchina, Russia
²⁸Institute of Theoretical and Experimental Physics (ITEP), Moscow, Russia
²⁹Institute of Nuclear Physics, Moscow State University (SINP MSU), Moscow, Russia
³⁰Institute for Nuclear Research of the Russian Academy of Sciences (INR RAN), Moscow, Russia
³¹Budker Institute of Nuclear Physics (SB RAS) and Novosibirsk State University, Novosibirsk, Russia
³²Institute for High Energy Physics (IHEP), Protvino, Russia
³³Universitat de Barcelona, Barcelona, Spain
³⁴Universidad de Santiago de Compostela, Santiago de Compostela, Spain
³⁵European Organization for Nuclear Research (CERN), Geneva, Switzerland
³⁶Ecole Polytechnique Fédérale de Lausanne (EPFL), Lausanne, Switzerland
³⁷Physik-Institut, Universität Zürich, Zürich, Switzerland
³⁸Nikhef National Institute for Subatomic Physics, Amsterdam, The Netherlands
³⁹Nikhef National Institute for Subatomic Physics and VU University Amsterdam, Amsterdam, The Netherlands
⁴⁰NSC Kharkiv Institute of Physics and Technology (NSC KIPT), Kharkiv, Ukraine
⁴¹Institute for Nuclear Research of the National Academy of Sciences (KINR), Kyiv, Ukraine
⁴²University of Birmingham, Birmingham, United Kingdom
⁴³H.H. Wills Physics Laboratory, University of Bristol, Bristol, United Kingdom
⁴⁴Cavendish Laboratory, University of Cambridge, Cambridge, United Kingdom
⁴⁵Department of Physics, University of Warwick, Coventry, United Kingdom
⁴⁶STFC Rutherford Appleton Laboratory, Didcot, United Kingdom
⁴⁷School of Physics and Astronomy, University of Edinburgh, Edinburgh, United Kingdom
⁴⁸School of Physics and Astronomy, University of Glasgow, Glasgow, United Kingdom
⁴⁹Oliver Lodge Laboratory, University of Liverpool, Liverpool, United Kingdom
⁵⁰Imperial College London, London, United Kingdom
⁵¹School of Physics and Astronomy, University of Manchester, Manchester, United Kingdom
⁵²Department of Physics, University of Oxford, Oxford, United Kingdom
⁵³Syracuse University, Syracuse, New York, USA
⁵⁴Pontifícia Universidade Católica do Rio de Janeiro (PUC-Rio),
Rio de Janeiro, Brazil (associated with Universidade Federal do Rio de Janeiro (UFRJ), Rio de Janeiro, Brazil)

⁵⁵*Institut für Physik, Universität Rostock, Rostock, Germany (associated with Physikalisches Institut, Ruprecht-Karls-Universität Heidelberg, Heidelberg, Germany)*

⁵⁶*Institute of Information Technology, COMSATS, Lahore, Pakistan (associated with Syracuse University, Syracuse, New York, USA)*

⁵⁷*University of Cincinnati, Cincinnati, Ohio, USA (associated with Syracuse University, Syracuse, New York, USA)*

^aAlso at LIFAELS, La Salle, Universitat Ramon Llull, Barcelona, Spain.

^bAlso at Università di Firenze, Firenze, Italy.

^cAlso at Università della Basilicata, Potenza, Italy.

^dAlso at Università di Modena e Reggio Emilia, Modena, Italy.

^eAlso at Università di Milano Bicocca, Milano, Italy.

^fAlso at Università di Bologna, Bologna, Italy.

^gAlso at Università di Roma Tor Vergata, Roma, Italy.

^hAlso at Università di Genova, Genova, Italy.

ⁱAlso at Università di Ferrara, Ferrara, Italy.

^jAlso at Università di Cagliari, Cagliari, Italy.

^kAlso at Hanoi University of Science, Hanoi, Vietnam.

^lAlso at Università di Bari, Bari, Italy.

^mAlso at Università di Roma La Sapienza, Roma, Italy.

ⁿAlso at Università di Urbino, Urbino, Italy.

^oAlso at Massachusetts Institute of Technology, Cambridge, MA, USA.

^pAlso at P.N. Lebedev Physical Institute, Russian Academy of Science (LPI RAS), Moscow, Russia.